COBEM 2023 27TH INTERNATIONAL CONGRESS OF MECHANICAL ENGENEERING

ABCM Brazilian Society of Mechanical Sciences and Engineering
27th ABCM International Congress of Mechanical Engineering
December 04-08, 2023, Florianópolis-SC, Brazil

# COB-2023-2296
# NUMERICAL ANALYSIS OF A TWO DIMENSIONAL COMPRESSIBLE FLUID FLOW OVER AN ASYMMETRIC GAP

**Thiago Freisleben Ribeiro Rezende**
**Felipe Oliveira Aguirre**
**Victor Barcelos Victorino**
**Marcello Augusto Faraco de Medeiros**
São Carlos School of Engineering - University of São Paulo. Av. Trabalhador são-carlense, 400, Arnold Schmidt. CEP 13566-590
thiago.freisleben@usp.br
felipe.aguirre@usp.br
barcelos.victorino@usp.br
marcello@sc.usp.br

***Abstract.*** *Boundary layer transition on fluid flows holds significant implications on the aerodynamic drag imposed on aircrafts due to the high coefficient of friction of turbulent boundary layers. The presence of gaps, small rectangular cavities, on the surface of the vehicle can accelerate transition. Stability analyses of the flow over gaps demonstrate that the interaction between two-dimensional unstable Rossiter modes and three-dimensional unstable centrifugal modes plays an important role in the boundary layer transition process. In this project, we evaluate the stability of two-dimensional compressible fluid flows past asymmetric rectangular gap configurations, i.e., gaps with trailing edge at a different height than the leading edge. We apply direct numerical simulation (DNS) of the compressible Navier-Stokes equations and linear stability theory (LST) using in-house algorithms. The analyses reveals that varying the trailing edge height of the gap affects the interaction between the two-dimensional mode and the mixing layer of the flow. Increases in the height of the trailing edge enhanced the stability of the two-dimensional mode, while lower trailing edges had the opposite effect and contributed to a significant increase in flow instability. It was observed that lower trailing edges also contributed to increased acoustic emission and circulation inside the gap.*

***Keywords:*** *Boundary Layer, Gaps, Direct Numerical Simulation, Linear Stability Theory, Compressible Flow.*

## 1. INTRODUCTION

Several processes in engineering involve the manipulation of fluid flows and are affected by the transition to turbulence. As presented in Davidson (2015), structural engineers need to predict turbulent wind gusts on bridges, while engine designers need to model the turbulent mixing of fuel and oxidizer. In aviation, predicting the boundary layer transition to turbulence is particularly important because the coefficient of friction in turbulent flows is larger than in laminar flows. Estimates in Reed *et al.* (1996), show that if the flow could be maintained in laminar regime along the entire wing span of a commercial aircraft, fuel savings of $25\%$ would be possible. Therefore, the control of the boundary layer transition has great potential in reducing airline operation costs and pollutant emissions.

Schlichting and Gersten (2016) present different factors that affect the stability of a boundary layer, among which is discussed the instability caused by the presence of wall roughness, a topic explored in this paper. In practice, any flow over a real surface is subject to surface imperfections. Recent studies by Crouch *et al.* (2020) demonstrate that the presence of rectangular cavities with dimensions on the order of magnitude of the boundary layer thickness (gaps) are sufficient to affect the transition to turbulence.

Rossiter (1964) proposes that the instability mechanism on the compressible flow over a cavity consists of acoustic feedback. In general, vortices are formed on the mixing layer after the leading edge and over the open space of the gap. Those vortices travel in the direction of the outer flow until they impact the trailing edge of the cavity. The impact produces an acoustic wave that re-excites the mixing layer producing more vortices and establishing the feedback loop.

On recent researches, Mathias (2021) delved into understanding the boundary layer transition process induced by gaps. The findings highlighted the essential role of the interaction between two-dimensional unstable Rossiter modes and three-dimensional unstable centrifugal modes in inducing the transition to turbulence. During the research, it was asked if the presence of asymmetry between the height of the leading edge and the trailing edge of the gap could have significant effects on the stability of the flow.

In this project, we aim to explore the effects of height asymmetry on the stability of a two-dimensional compressible fluid flow over a rectangular gap. With the study, we seek to provide some understanding of the physical phenomena observed and bring possible engineering solutions for controlling the stability of a flow over a real gap.

## 2. METHODOLOGY

In this paper, we perform multiple two-dimensional simulations of flows over rectangular gaps with varying trailing edge height. Figure 1 shows the geometric parameters of the problem and the direction of the free stream. The depth of the gap is defined as $D$ and the length as $L$. The difference in height between the leading and the trailing edge is represented by the variable $s$. At the configuration presented in Fig. 1, a boundary layer is formed upstream of the gap and its displacement thickness at the leading edge is defined as $\delta^*$ (not shown).

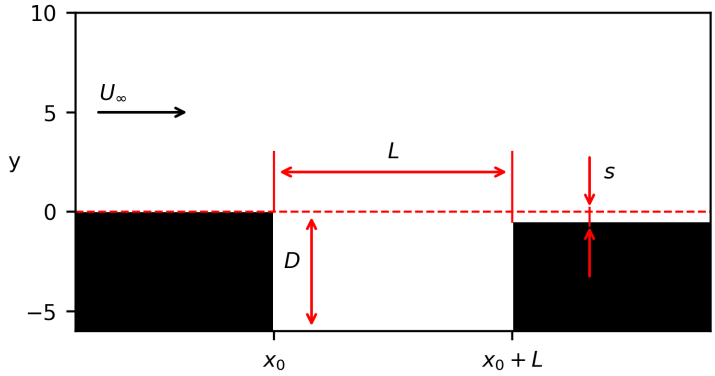


Figure 1. Geometrical variables. The displacement thickness of the boundary layer at the leading edge of the cavity is defined with the notation $\delta^*$ (not shown in the figure).

To construct the physical domain, the position of the leading edge of the cavity is calculated so that the displacement thickness of the laminar boundary layer is unitary at this point ($\delta^* = 1$ at $x = x_0$). The strategy allows for scaling the length measurements of the entire domain, i.e., all geometrical lengths of the simulation are non-dimensional and measured as a function of the boundary layer displacement thickness at the leading edge of the gap ($\delta^*$). With this approach, the value obtained for the position of the leading edge ($x_0$), considering the parameters of Tab. 1, is $x_0 \approx 248.1\delta^* = 248.1$. The lower boundary on the $y$ axis is the depth of the cavity ($y_{min} = -D$) and the upper boundary is approximately two times the maximum turbulent boundary layer displacement thickness expected on the domain ($y_{max} \approx 28.9$). The length of the domain downstream of the cavity was arbitrary, with sufficient size to capture the phenomena of interest for this study ($x_{max} = 500$). Finally, a buffer zone is added at the boundaries of the physical domain, a region where a Selective Frequency Damping (SFD) method is applied to avoid reflection of waves coming from the physical domain, as described in Mathias (2021). A free slip condition was applied at the wall in the region before the physical domain to fix the position of the formation of the boundary layer. The complete simulation domain and some of the applied boundary conditions are presented in Fig. 2.

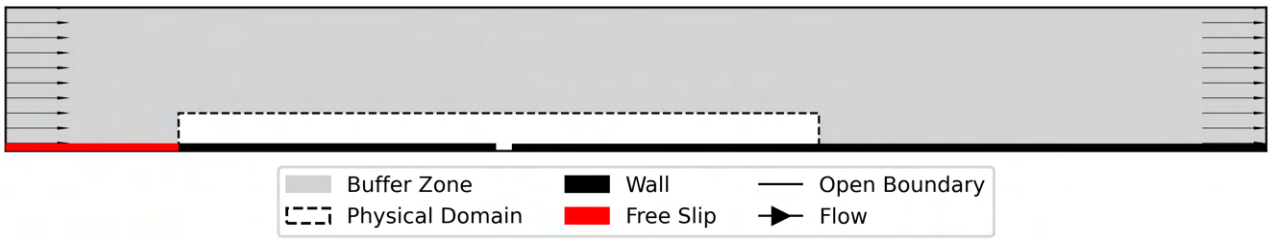


Figure 2. Simulation domain and boundary conditions.

The simulation domain is filled with a rectangular structured mesh, and the strategy to calculate the distances between the points for the finite differences method (horizontal distance $l_x$ and vertical distance $l_y$) was based on previous studies carried out with similar configurations (Mathias (2021)). The distribution of distances between points of the mesh is shown in Fig. 3 . In particular, the leading edge (point of detachment of the boundary layer) and the trailing edge (impact and reattachment of the boundary layer) were the regions of greatest mesh refinement, followed by the region immediately downstream of the cavity. A horizontal mesh refinement was applied in the region at the beginning of the physical domain to ensure good representation of the boundary layer formation. The mesh contains $N_x = 1027$ points on the horizontal axis and $N_y = 364$ points on the vertical axis, the smallest distances are $dx = 0.12$ and $dy = 0.048$ and they are inside the cavity.

The mesh was validated by means of convergence analysis. The symmetric gap ($s = 0$) configuration was simulated using the mesh described above and a mesh twice as refined, the results were corresponding and the mesh was considered valid for all other small geometry variations analyzed in this study.

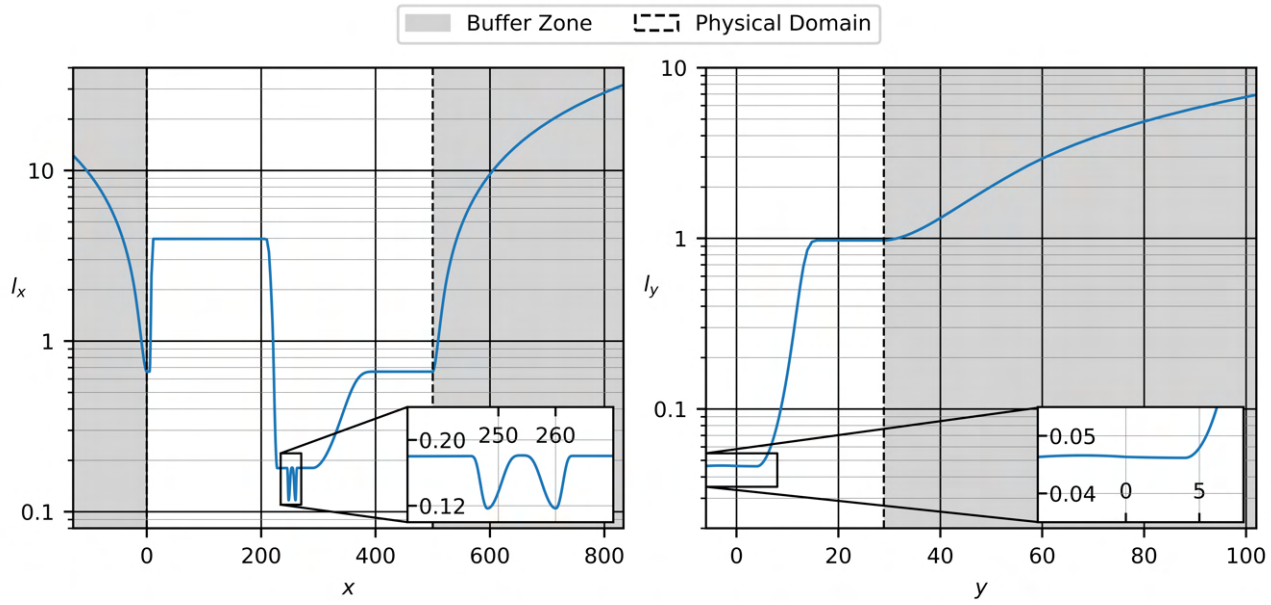


Figure 3. Distribution of distances between mesh points ($l_x$,$l_y$) within the structured mesh for finite differences.

The simulation campaign is carried out by fixing the parameters of the Tab. 1 and varying only the height of the trailing edge with intervals of $\Delta s = 0.1$ in the range $s \in [-1, 1]$. The Reynolds number is calculated considering the laminar boundary layer displacement thickness at the leading edge of the cavity as a reference length. The temperature is measured in Kelvin. In particular, the geometry parameters $D$ and $L$ and the variable $s$ are all non-dimensional and measured as multiples of the boundary layer displacement thickness at the leading edge, which is unitary ($\delta^* = 1$) as described above.

Table 1. Parameters for simulations.

| **Parameter** | **Value** |
|---|---|
| Ma | 0.5 |
| $\mathrm{Re}^{\delta^*}$ | 734 |
| $\mathrm{T}_0$, Kelvin | 300 |
| $\mathrm{D}^{(1)}$ | 6 |
| $\mathrm{L}^{(1)}$ | 12 |

$^{(1)}$ Non-dimensional geometry parameters.

To illustrate the varying height of the trailing edge, Fig. 4 shows the geometry of three distinct cases. The value of $s$ is positive if the trailing edge is above the leading edge and negative if it is below. An algorithm developed in-house was used to solve the compressible Navier-Stokes equations by the method of Direct Numerical Simulation (DNS) and to calculate the stability of the flows with Linear Stability Theory (LST). The tools used in the calculations and the optimization strategies are described in detail in Mathias (2021).

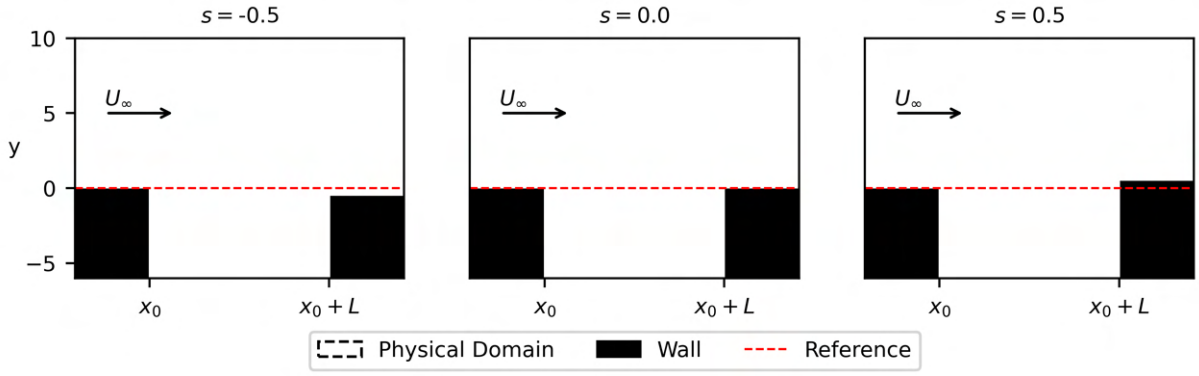


Figure 4. Geometry set-up of three different cases. The variable $s$ is positive if the trailing edge is higher than the leading edge, and negative if it is lower.

Finally, one probe point, two probe lines and one probe surface were positioned on the mesh, as shown in Fig. 5. The point *P* is positioned at a distance $d = \delta^* = 1$ above the trailing edge of the cavity and records the temporal velocity signal at this point. The signal is then processed and its spectrum gives information about the dominant frequencies and amplitudes of the velocity fluctuations within the flow. Moreover, the circulation inside the cavity is calculated in the region $S$ according to the surface integral on Eq. (1). The procedure allows for quantifying the circulation of fluid in this region and provides information about how the circulation is affected by the geometry changes. The position of region $S$ and its horizontal length were selected so that it captures the main circulation on the second half of the cavity. The upper boundary of region $S$ is aligned with the trailing edge of the gap for negative asymmetries ($s < 0$) and aligned with the leading edge for positive asymmetries ($s > 0$) to avoid inclusion of the vorticity of the mixing layer on the integral on Eq. (1).

$$\Gamma = \int\int_S \omega ds, \tag{1}$$

At last, curves *SL* and *Ac* are used to evaluate the acoustic properties of the cavity. In particular, curve $SL$ is used to quantify the sound sources on the shear layer of the flow through the computation of the integral on Eq. (2). Curve $SL$ is positioned at three quarters of the length of cavity and has sufficient size to capture the shear layer of the flow. On the other hand, the energy of the pressure waves emitted by the cavity is quantified by the integral presented on Eq. (3). Curve $Ac$ was defined as an arc of circle with center fixed at the trailing edge of the gap with symmetrical configuration ($s = 0$). The radius of the arc corresponds to two times the length of the cavity ($R = 2L$). The geometry of the arc was selected as to capture stable pressure fluctuations and avoid interaction with the boundary layer downstream of the gap. The combined analysis of the shear layer sound sources and the pressure fluctuations allows for quantifying the acoustic feedback mechanism of the cavity. This sound emission analysis is inspired on a model described in Howe (2004).

$$E_{SL} = \int_{SL} |\nabla \cdot (\omega' \times V')| ds, \tag{2}$$

$$E_{Ac} = \int_{Ac} |p'|^2 ds, \tag{3}$$

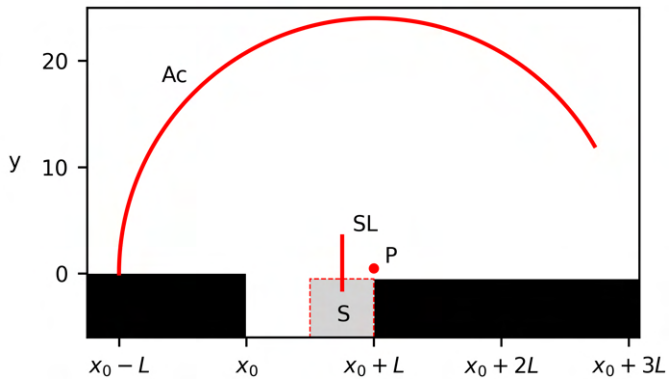


Figure 5. Probe point, probe curves and probe surface. Point *P* captures the temporal velocity signal, curves $SL$ and $Ac$ evaluate acoustic emissions and region $S$ is used to compute circulation on the mean flow.

## 3. RESULTS

### 3.1 Direct Numerical Simulation

Direct Numerical Simulations of the flow over the three geometries shown in Fig. 4 ($s = [-0.5, 0, +0.5]$) point out that changing the height of the trailing edge drastically affects the stability of the flow, the results are presented on Fig. 6. At the left of Fig. 6, the velocity fields of the mean flows indicate the existence of circulation inside the cavity. In particular, the flow fields point out that the circulation increases as the height of the trailing edge is lowered. On the other hand, the graphs at the center and at the right of Fig. 6 compare the velocity fluctuations registered at point *P* presented on Fig. 5 (at a distance of $d = \delta^*$ above the trailing edge of the gap). The graphs show that the gap with positive $s$ damped the limit cycle oscillations observed in the other two cases. The negative $s$ configuration presented higher amplitude oscillations and introduced other frequencies to the signal. Therefore, increasing the height of the trailing edge of the gap had a stabilizing effect.

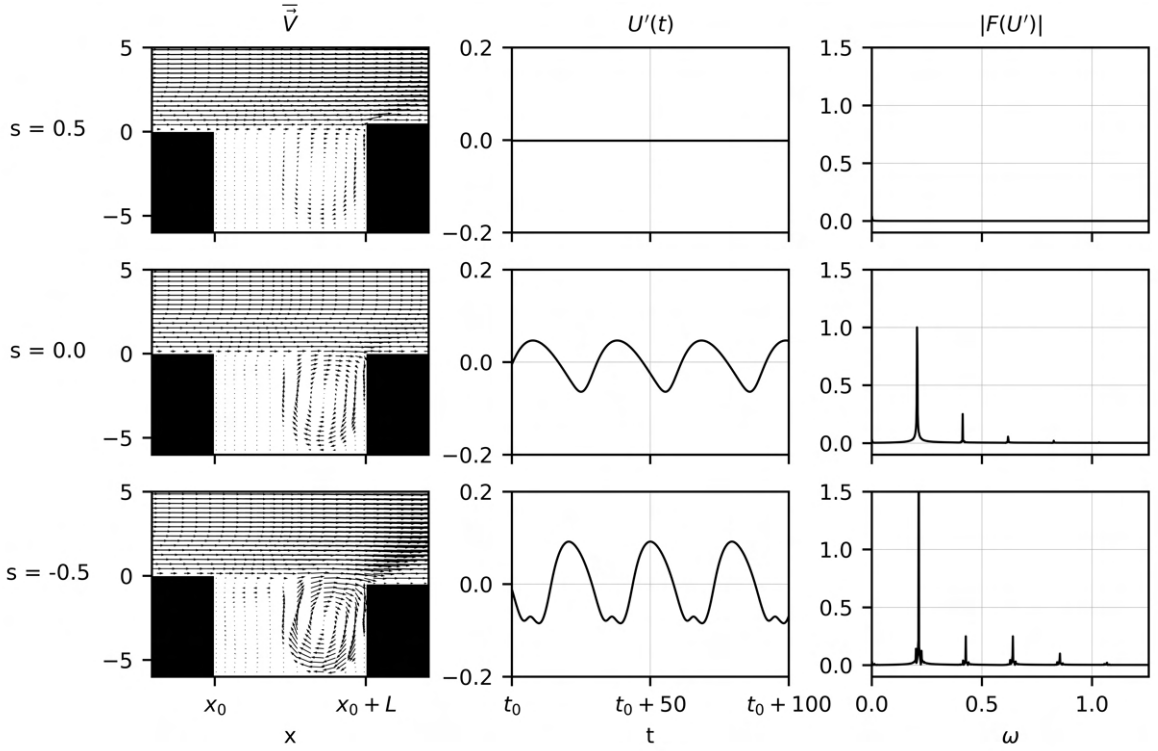


Figure 6. On the left, mean velocity field for three $s$ values. At the center, horizontal velocity fluctuations on a probe at a distance of $d = \delta^*$ above the trailing edge of the gap. On the right, spectrum of the signal.

The analysis presented for the three cases in Fig. 6 was extended to the interval $s \in [-1, 1]$ with variations of $\Delta s = 0.1$ and it was confirmed that the increase of the trailing edge contributed to stabilize the flow over the gap, reducing the amplitude of the oscillations. In particular, the stability limit was found around $s = 0.3$, above which the flow becomes stable and non-oscillatory.

In addition, a more detailed inspection of the mean velocity field in the vicinity of the trailing edge was carried out, the results are shown in Fig. 7. Significant changes are observed in the angle and magnitude of the flow velocity that impinges on the trailing edge. In particular, it is observed that a decrease in the height of the trailing edge in the interval $-0.8 < s < 0$ is associated with a curvature of the flow and possibly with an increase in the velocity of the fluid before impact with the wall, which may be related to an increase in acoustic emission in these configurations. However, greater reductions in the trailing edge in the interval $s < -0.8$ caused the point of reattachment of the boundary layer to move downstream of the cavity and generated a region of recirculation above the trailing edge. Finally, it was generally observed that reductions in the trailing edge ($s < 0$) contributed to the formation of an inflectional velocity profile downstream of the cavity. As discussed in Schlichting and Gersten (2016), the inflection of the velocity profiles is a sufficient condition for the amplification of disturbance waves in the flow, i.e., the inflectional velocity profiles indicate once more that lower trailing edges were associated to an increase in flow instability.

Finally, a group of flow properties were recorded for all geometry configurations in the range $s \in [-1, 1]$ to quantify the changes in flow behavior associated with the geometry changes of the trailing edge of the gap. The results are shown in Fig. 8. All the quantities shown in the graph are divided by the value obtained in the symmetrical configuration ($s = 0$), so that all the variables have unitary value at the point $s = 0$. In addition, some curves were interrupted at the point $s = 0.2$, as this corresponds to the stability threshold found in this research and is therefore a point of discontinuity. The interrupted curves have values that tend to zero for $s \geq 0.3$, except for the ratio $E_{Ac}/E_{SL}$, which becomes very large and was also not shown.

In particular, the variable $\Gamma$ represents the circulation in the second half of the cavity, as shown in Fig. 5. Figure 8 shows that the circulation increases with a decrease in the trailing edge height and that there is a discontinuity in the vicinity of the value $s = -0.8$. The increase in circulation may contribute to change the angle and intensity of the impact of the fluid on the trailing edge, which may influence the stability of the flow and the sound emission capability of the cavity as discussed previously.

The variable $\overline{U}_P$ represents the mean flow velocity at *P* point of Fig. 5. By analyzing Fig. 8, it is noted that a reduction in the height of the trailing edge had the effect of reducing the mean velocity of the flow, while increasing the height had the effect of increasing the mean velocity of the fluid at point *P*. This result is to be expected, since configurations with values of $s > 0$ imply a contraction of the flow, which may contribute to the increase in velocity.

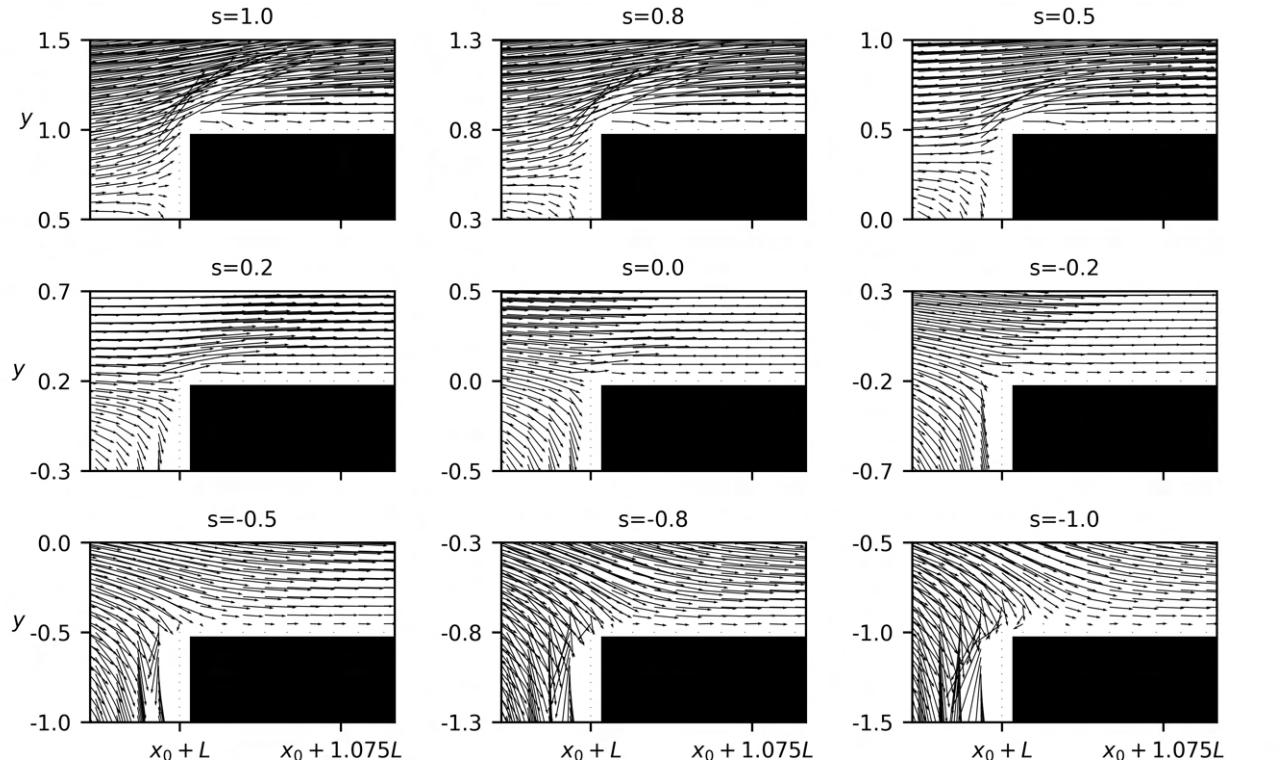


Figure 7. Velocity field of the mean flow near the trailing edge in nine different configurations. Lower trailing edges favored the impact of the flow and contributed to the formation of an inflexional velocity profile downstream of the gap.

On the other hand, the variables $\omega_{peak}$ and $\alpha_{peak}$ are associated with the spectrum of the velocity signal obtained at point *P*. In particular, $\omega_{peak}$ represents the dominant frequency in the spectrum, while $\alpha_{peak}$ corresponds to the amplitude of the peak associated with the dominant frequency. It is noticeable from Fig. 8 that the dominant frequency is little altered by the geometry changes. On the other hand, the amplitude of the dominant frequency increases until around $s = -0.5$, then there is a sharp drop, a recovery and then a gradual drop with decreasing trailing edge heights. The discontinuity observed in the vicinity of point $s = -0.6$ is possibly associated with the appearance of a second unstable mode in the flow (shown later in the next section in Fig. 9), which contributes to a distribution of the spectrum and consequently a reduction in the peak associated with the first unstable mode.

Finally, the variables $E_{Ac}$ and $E_{SL}$ are used to quantify the cavity's acoustic emission capacity, as presented in the previous section and illustrated in Fig. 5. In particular, Fig. 8 shows that both the intensity of the pressure fluctuations and the sound sources in the shear layer are intensified by a reduction in the trailing edge height ($s < 0$). Again, there is a discontinuity in the vicinity of $s = -0.8$, a phenomenon that may be associated with the sudden shift of the boundary layer reattachment point, which becomes downstream of the cavity's trailing edge for very negative values of $s$ around $s < -0.8$, as discussed earlier and presented in Fig. 7. Lastly, Fig. 8 presents a curve for the ratio $E_{Ac}/E_{SL}$, which can be considered as a way of measuring the efficiency of the sound emission mechanism for the cavity in each configuration of $s$. It is noted that the ratio decreases as the trailing edge of the cavity lowers, which indicates that, although the cavity produces more sound as the trailing edge is lowered, the sound emission process seems to be more efficient for higher trailing edges.

### 3.2 Linear Stability Theory

In order to further investigate the stability of the cavity on multiple configurations, a campaign of linear stability calculations (tools presented in Mathias (2021)) of gap configurations with values of $s$ in the range $s \in [-1, 1]$ and with $\Delta s = 0.1$ confirm that the stability of the flow is directly affected by the height of the trailing edge of the gap.

The graph on the left of Fig. 9 shows the distribution of the complex eigenvalues of the system, which is symmetric about the $x$ axis. Each color represents the eigenvalues of the flow for one geometry configuration ($s$). It is remarkable the presence of a group of eigenvalues with frequencies around $\sigma_i(R1) \approx \pm 0.21$ and another group with frequencies around $\sigma_i(R2) \approx \pm 0.32$. These frequencies are characteristic of the Rossiter 1 and Rossiter 2 modes, respectively. In this study, the Rossiter 1 mode was dominant for all trailing edge height configurations. In particular, it is noted that the real part of the Rossiter modes, i.e., the amplification of the disturbance waves, is shifted with the change of the trailing edge height. The graph on the right of Fig. 9 demonstrates the amplification ($\sigma_r$) as a function of $s$. It is remarkable that

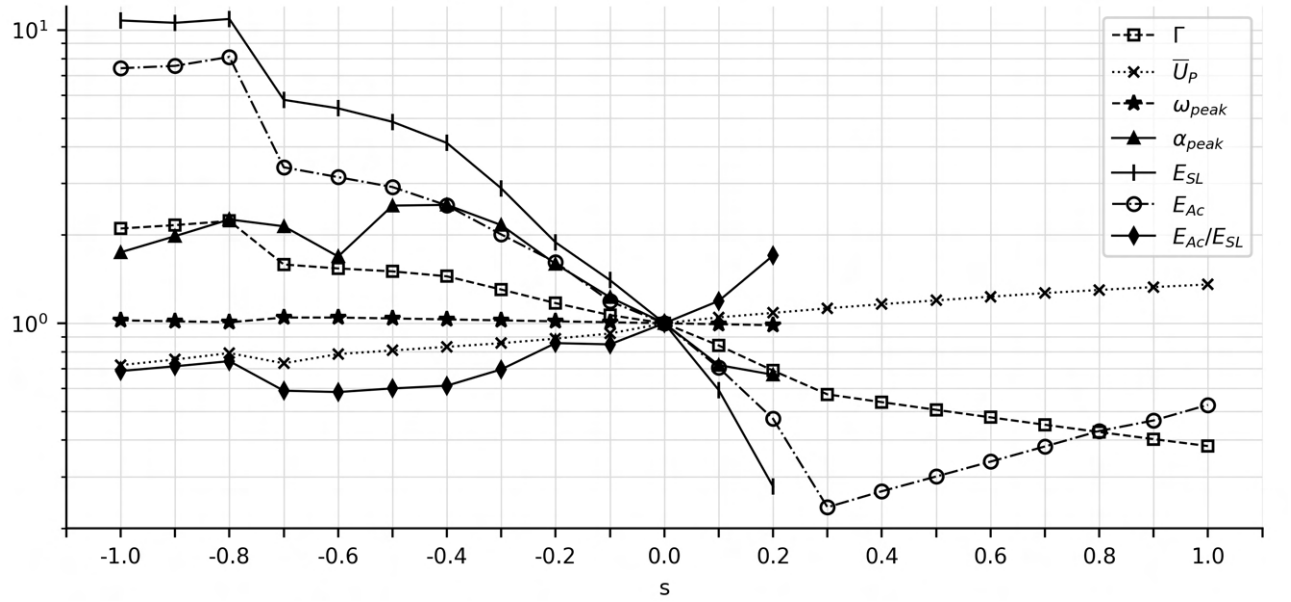


Figure 8. Physical properties of the flow as a function of the height difference at the trailing edge. Results are divided by the reference value obtained for the symmetrical cavity ($s = 0$).

an increase in the trailing edge height is generally associated with a decrease on the real part of the eigenvalues, which implies an increase on the stability of the flow. In fact, Fig. 9 demonstrates that for $s \geq 0.3$ all eigenvalues have real part lower than zero and thus the flow over the cavity becomes stable for all $s \geq 0.3$. The linear stability analysis agrees well with the results obtained via Direct Numerical Stimulation presented earlier. Furthermore, Fig. 9 shows that the Rossiter mode 2 is also highly affected by the trailing edge height. In particular, it is observed that this mode becomes unstable for $s \leq 0.6$ and that this configuration also corresponds to a maximum instability of the Rossiter 1 mode. After the peak instability of the Rossiter mode 1 around $s = -0.6$ it is noted that the mode starts to settle as the trailing edge is further decreased, which can also be associated to the behavior of curve $\alpha_{peak}$ obtained via Direct Numerical Simulation and presented earlier on Fig. 8.

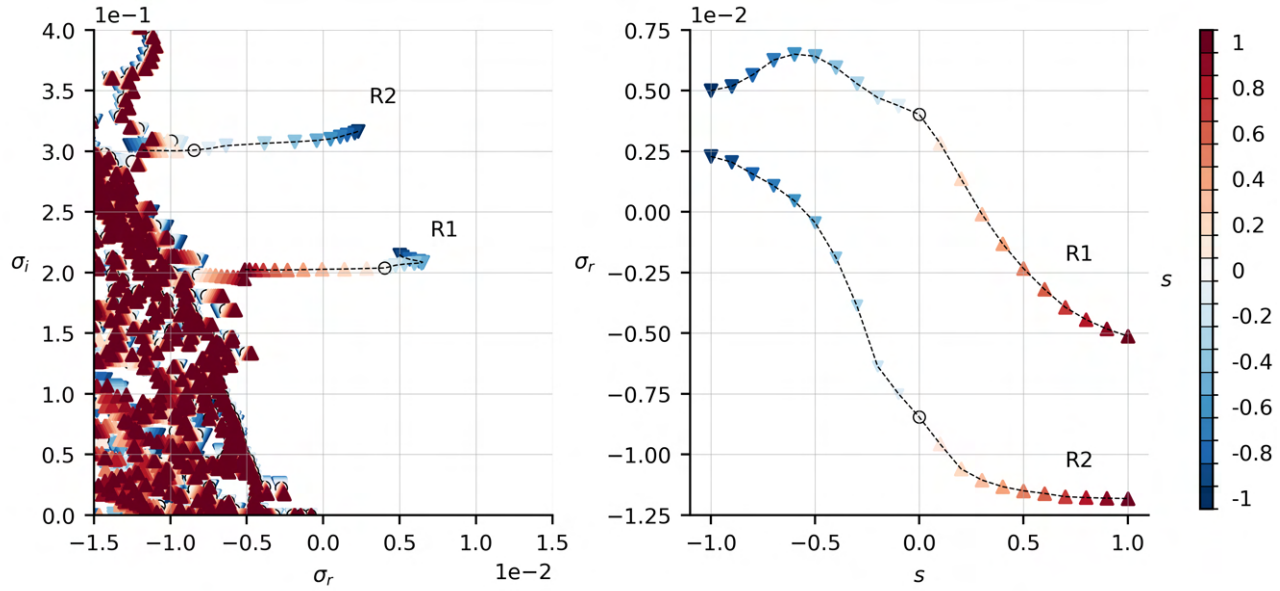


Figure 9. Eigenvalues of the flow and amplification as a function of $s$. Increasing $s$ reduced the amplifications. The flow is stable for $s > 0.3$.

Finally, an analysis of the eigenfunctions associated with Rossiter modes 1 and 2 allows for the identification of the regions on the flow where the oscillations are to be amplified. Figure 10 shows the shapes of the eigenfunctions associated with the unstable Rossiter modes on an arbitrary phase. Moreover, Fig. 10 has five lines and each line corresponds to a fixed value of $s$. The Rossiter mode 2 is stable for the configurations where $s = [-0.2, 0, 0.2]$ and thus the eigenfunctions

associated with this mode were not displayed for those geometries.

One observes periodic amplification peaks located in the region of the mixing layer that extend from the open space over the gap to the region downstream of the cavity. In particular, it is noted that reducing the height of the trailing edge of the gap concentrated the peaks of the eigenfunctions downstream of the cavity. Furthermore, Fig. 10 also demonstrates that for the Rossiter 1 eigenfunctions there is generally one wavelength of the mode on the open space over the cavity. On the other hand, for the Rossiter 2 mode there are two wavelengths over the cavity. This behavior is to be expected for the Rossiter mode and is related to the acoustic feedback mechanism described earlier.

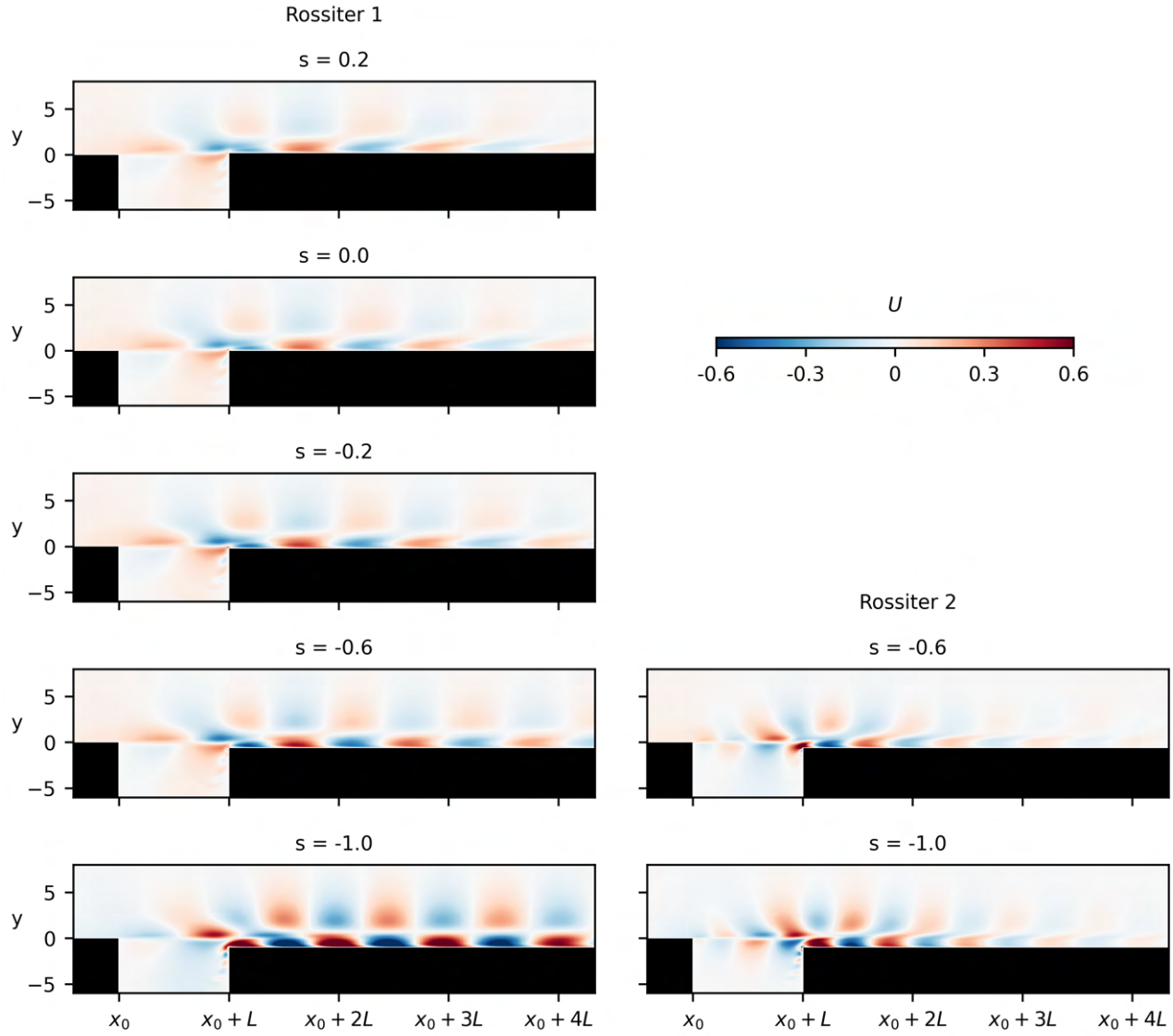


Figure 10. Eigenfunctions of the unstable modes in five different configurations. Lower trailing edges made eigenfunction peaks move downstream.

## 4. ANALYSIS IN PROGRESS

Currently, the focus of this study is to present a robust explanation for the observed phenomena, i.e., to demonstrate the physical mechanism responsible for changing the stability of the flow over the gap with the change in the height of the trailing edge. Investigations point out that at least three mechanisms may be present in establishing the instability. On the one hand, changing the height of the trailing edge can affect the intensity of vortex formation in the mixing layer and circulation inside the cavity, which may influence the stability of the boundary layer. The second phenomenon consists in the mechanism of acoustic wave formation, the study shows that the change in the height of the trailing edge of the gap alters the angle and velocity of the impact of flow on the trailing edge, which can bring about changes in the conversion between vorticity and acoustic waves. A third instability mechanism may be related to the possible formation of an adverse pressure gradient downstream of the gap for negative values of $s$. These phenomena still need to be further explored.

In parallel, a study is being conducted to determine if the effect found can be generalized to other combinations of the parameters in Tab. 1, that is, to verify if the stabilizing effect of increasing the height of the trailing edge can be observed in a generic cavity with other dimensions and Ma and $\text{Re}^{\delta^*}$ parameters.

Finally, this project will seek to perform three-dimensional simulations of some critical cases selected from the two-dimensional simulations. The goal is to verify if the trend of flow stabilization with increasing trailing edge height is also observed in 3D cases and, in particular, to analyze the effect of height change on the intensity of the unsteady centrifugal modes documented in Bres and Colonius (2008).

## 5. CONCLUSION

The study presented in this paper demonstrates that, in the context of a compressible fluid flow over a rectangular cavity, the presence of an asymmetry between the height of the leading and trailing edges of the cavity can have significant effects on the stability of the flow. In particular, the results of the campaign of two-dimensional direct numerical simulations indicates that the presence of negative asymmetry ($s < 0$) can induce an increase in circulation inside the cavity and that the phenomenon may be associated with a change in the angle and intensity of the flow velocity that impacts the trailing edge. In addition, lower trailing edges were associated to an intensification of the vortices formed in the mixing layer and an increase in acoustic emission. On the other hand, the opposite effects were observed for positive asymmetry configurations ($s > 0$), where it was noted a reduction on circulation, pressure fluctuations and vortices formation on the mixing layer. In particular, values of $s \geq 0.3$ stabilized the flow over the gap. Finally, the sound emission was greater for lower trailing edges, but the efficiency of the sound emission mechanism seemed to be improved for positive asymmetries.

Moreover, the campaign of linear stability analyses confirmed that an asymmetry between the leading and the trailing edge of the cavity can play an important role on the stability of the flow. In general, negative asymmetries ($s < 0$) increased the real part of the Rossiter eigenvalues leading to a more unstable flow. On the other hand, positive asymmetries ($s > 0$) contributed to a decrease on the real part of the eigenvalues. In particular, values of $s \geq 0.3$ lead to eigenvalues with negatives real parts, which again indicates the stabilization of the flow over the gap. At last, the analyses also showed that the dominant modes are the Rossiter modes, and that the eigenfunctions associated with these modes manifest themselves mainly in the mixing layer of the flow, as in the case of a symmetrical rectangular cavity. The results obtained using Linear Stability Theory agreed well with those obtained via Direct Numerical Simulations.

Finally, the significant changes noted on the two-dimensional circulation and stability due to the presence of height asymmetry between the leading and trailing edge give some indication that the three-dimensional centrifugal mode may also be significantly influenced by the geometrical asymmetry. If so, the results suggest that the boundary layer transition process on a more complex three-dimensional flow over a real cavity may be accelerated or delayed depending on the height asymmetry between the edges. Nevertheless, future investigations are still needed on the behavior of the three-dimensional flow over the asymmetrical gap and its implications on boundary layer transition.

## 6. ACKNOWLEDGEMENTS

We would like to thank the Coordenação de Aperfeiçoamento de Pessoal de Nível Superior (CAPES)- Programa de Excelência Acadêmica (PROEX) - Brasil for Financial Support. T.F.R.R. thanks the São Paulo Research Foundation (FAPESP) grant no. 2023/08223-0. M.A.F.M. thanks the National Council for Scientific and Technological Development (CNPq/Brazil) grant no.307956/2019-9), the São Paulo Research Foundation (FAPESP) grant no. 2019/15336-7 and the US Air Force Office of Scientific Research (AFOSR) for grants FA9550-18-1-0112 and FA9550-23-1-0030, managed by Dr. Roger Greenwood. We thank the Center for Mathematical Sciences Applied to Industry (CeMEAI) funded by São Paulo Research Foundation (FAPESP/Brazil), grant 2013/07375-0, for access to the Euler cluster, led by Prof. José Alberto Cuminato. This work used resources of the "Centro Nacional de Processamento de Alto Desempenho em São Paulo (CENAPAD-SP)."

## 7. REFERENCES

Bres, G.A. and Colonius, T., 2008. "Three-dimensional instabilities in compressible flow over open cavities". *Journal of Fluid Mechanics*, Vol. 599, pp. 309–339.

Crouch, J.D., Kosorygin, V.S. and Sutanto, M.I., 2020. "Modeling gap effects on transition dominated by tollmien-schlichting instability". In *AIAA Aviation 2020 Forum*. p. 3075.

Davidson, P.A., 2015. *Turbulence: an introduction for scientists and engineers*. Oxford university press.

Howe, M., 2004. "Mechanism of sound generation by low mach number flow over a wall cavity". *Journal of sound and vibration*, Vol. 273, No. 1-2, pp. 103–123.

Mathias, M.S., 2021. *Computational study of the hydrodynamic stability of gaps and cavities in a subsonic compressible boundary layer*. Ph.D. thesis, Universidade de São Paulo.

Reed, H.L., Saric, W.S. and Arnal, D., 1996. "Linear stability theory applied to boundary layers". *Annual review of fluid*

*mechanics*, Vol. 28, No. 1, pp. 389–428.
Rossiter, J., 1964. "Wind-tunnel experiments on the flow over rectangular cavities at subsonic and transonic speeds".
Schlichting, H. and Gersten, K., 2016. *Boundary-layer theory*. springer.

## 8. RESPONSIBILITY NOTICE

The authors are solely responsible for the printed material included in this paper.